Available online at www.sciencedirect.com
SCIENCE DIRECT
Biochemical and Biophysical Research Communications 346 (2006) 938–945
BBRC
www.elsevier.com/locate/ybbrc

Afterhyperpolarization improves spike programming through lowering threshold potentials and refractory periods mediated by voltage-gated sodium channels ☆

Na Chen, Xin Chen, Jiandong Yu, Jinhui Wang *

State Key Lab for Brain and Cognitive Sciences, National Lab for Protein Sciences, Institute of Biophysics Chinese Academy of Sciences, Beijing 100101, China

Received 24 May 2006
Available online 9 June 2006

Abstract

Neurons program various patterns of sequential spikes as neural codes to guide animal behavior. Studies show that spike programming (capacity and timing precision) is influenced by inhibitory synaptic inputs and membrane afterhyperpolarization (AHP). Less is clear about how these inhibitory components regulate spike programming, which we investigated at the cortical neurons. Whole-cell current-clamp recording for action potentials and single channel recording for voltage-gated sodium channels (VGSC) were conducted at regular-spiking and fast-spiking neurons in the cortical slices. With quantifying the threshold potentials and refractory periods of *sequential spikes*, we found that fast-spiking neurons expressing AHP possess lower threshold potentials and shorter refractory periods, and the hyperpolarization pulse immediately after each of spikes lowers threshold potentials and shortens refractory periods at regular-spiking neurons. Moreover, the hyperpolarization pulses shorten the refractory periods for VGSC reactivation and threshold potentials for its sequential activation. Our data indicate that inhibitory components immediately after spikes, such as AHP and recurrent inhibition, improve spike capacity and timing precision via lowering the refractory periods and threshold potentials mediated by voltage-gated sodium channels.

Keywords: Action potential; Spike timing precision; Spike capacity; Refractory period; Threshold potential; Hyperpolarization and neurons

The precise behaviors (e.g., perception, motion, and cognition) are controlled by the meaningful signals programmed at neurons and synapses under the physiological conditions. The molecular bases of such behaviors were studied [1,2]. Less is known about how the neurons program the neural codes precisely. Sequential spikes, likely the digital signals from silicon-based switch, are thought of the preferred candidates for neural computations [3–8]. Spike timing is also critical [9,10] since precise and loyal spike patterns signify neuronal events in meaningful and memorable manner. It is pivotal to uncover mechanisms navigating spike timing precision and capacity.

The spike patterns are believed to be modulated by synapse dynamics [6,7,11,12], and by membrane potentials in experiments [4,13–16] or in simulation model [17–19]. Afterhyperpolarization (AHP) generated from the potassium channels and recurrent inhibitory synapses affects neuronal excitability as well as spike timing [20–26]. We found that threshold potentials and refractory periods control spike programming [27]. Do membrane potentials and synapse dynamics influence the programming of sequential spikes in direct manner or via altering the refractory periods and threshold potentials mediated by voltage-gated sodium channel (VGSC)?

☆ *Abbreviations:* Vr, resting membrane potential; Vm, membrane potential; Vts, threshold potential; Vts-Vr, the difference between threshold potential and resting membrane potential; RP, refractory period; AHP, afterhyperpolarization; RSN, regular-spiking neuron; FSN, fast-spiking neuron; ISI, inter-spike interval; SDST, standard deviation of spike timing; VGSC, voltage-gated sodium channels.

* Corresponding author. Fax: +86 10 64888472.
E-mail address: jhw@sun5.ibp.ac.cn (J. Wang).

0006-291X/$ - see front matter © 2006 Elsevier Inc. All rights reserved.
doi:10.1016/j.bbrc.2006.06.003

To questions above, we investigated the influences of afterhyperpolarization on sequential spikes as well as their threshold potentials and refractory periods at the fast-spiking neurons (FSN) with expressing AHP and regular-spiking neurons (RSN) without AHP in cortical slices by whole-cell clamp recordings. We also examined such influences by recording the activities of single VGSCs.

Materials and methods

Brain slices. Cortical slices (400 μm) were prepared from Sprague-Dawley rats (postnatal day16–22) that were anesthetized by injecting pentobarbital (50 mg/kg) and decapitated with a guillotine. The slices were cut with a Vibratome in the modified and oxygenized (95% O_2/5% CO_2) artificial cerebrospinal fluid (mM: 124 NaCl, 3 KCl, 1.2 NaH_2PO_4, 26 $NaHCO_3$, 0.5 $CaCl_2$, 5 $MgSO_4$, 10 dextrose, and 5 Hepes, pH 7.35) at 4 °C, and then were held in the normal oxygenated ACSF (mM: 124 NaCl, 3 KCl, 1.2 NaH_2PO_4, 26 $NaHCO_3$, 2.4 $CaCl_2$, 1.3 $MgSO_4$, 10 dextrose, and 5 Hepes, pH 7.35) at 24 °C for 1–2 h before experiments. A slice was transferred to the submersion chamber (Warner RC-26G) that was perfused with the normal ACSF at 31 °C for the whole-cell recordings [27]. Chemicals were purchased from Fisher Scientific. The procedures were approved by IACUC in Beijing, China.

Neuron selection. Neurons in the layer II–III of sensorimotor cortex were recorded. Regular-spiking neurons (RSN) show pyramidal-like soma and an apical dendrite; and fast-spiking neurons (FSN) are round with multiple processes under DIC optics (Nikon FN-E600). RSN and FSN show different properties in the response to current pulses [27–29].

Whole-cell recording. Action potentials were recorded with multi-clamp 700B, and inputted into pClamp 9 (Axon Instrument Inc., Foster CA, USA) for data acquisition and analyses. Output bandwidth was set at 3 kHz. Spike patterns and modulation at RSN and FSN were studied by using the simulated pulses or currents (depolarization, hyperpolarization or mixed pulses). The intensity of currents for evoking sequential spikes equals the threshold pulse (10 ms) of eliciting a single spike. The standard pipette solution contains (mM) 150 K-gluconate, 5 NaCl, 10 Hepes, 0.4 EGTA, 4 Mg-ATP, 0.5 Tris–GTP, and 4 Na-phosphocreatine (pH 7.4, adjusted by 2 M KOH). Fresh pipette solution was filtered with 0.1 μm centrifuge filter. Its osmolarity was 295–305 mOs mol; and pipette resistance was 6–8 MΩ.

Neuronal intrinsic properties. The threshold potentials and refractory periods of sequential spikes were measured and defined in previous study [27]. Inter-spike intervals (ISI, an index of spike capacity) are the duration between a pair of spikes; and the standard deviation of spike timing (SDST, an index of spike precision) is the standard deviation of spike lock-phase. Data were analyzed if Vr was above −60 mV at the recorded FSN and −67 mV at RSN. The criteria for the acceptation of each experiment also included less than 5% changes in Vr, spike magnitude, and input resistance throughout each of experiments [27]. The values of Vts, RP, ISI, and SDST are presented as means ± SE. The comparisons between a pair of treatments were done by *t*-test.

Single-channel recording. The signals from VGSC were recorded in cell-attached configuration with multi-clamp 700B and pClamp-9 at neurons in cortical slices. Seal resistance was above 20 GΩ, and pipette resistance was 10–15 MΩ. Pipette solution contains (mM) 120 NaCl, 2 MgCl2, 10 Hepes, 30 TEA, and 0.1 mibefradil. TEA and mibefradil were used to block voltage-gated potassium and type-T calcium channels, respectively. Threshold potentials for VGSC activation were measured when adding negative voltage pulses (4 ms) into the recording pipettes; and refractory periods for VGSC reactivation were measured when changing inter-pulse intervals (IPI) in 6–8 ms. We also measured ARP for VGSC reactivation by raising depolarization intensity. The events of single VGSCs in Fig. 5 are summated.

Results

The strategy for addressing the mechanisms underlying the influences of AHP on spike capacity and timing precision was comparing the influences of the given inputs on spike patterns and intrinsic properties at the neurons with and without expressing AHP. This approach is based on a principle of occlusion that spike programming at the neurons expressing natural AHP should not be affected significantly by a given AHP.

Spike programming at neurons with and without AHP

The current pulses integrated from hundreds of excitatory synapses were injected into RSN and FSN to elicit sequential spikes. Fig. 1 shows the influences of excitatory inputs on inter-spike intervals (ISI) and standard deviation of spike timing (SDST). To the given inputs (260 ms) at threshold intensity that was the value of 5 ms pulse for a single spike, the number and timing of spikes are better at FSN than RSN. The values for $SDST_1$ to $SDST_4$ are 1.45 ± 0.2, 2.24 ± 0.26, 3.39 ± 0.5, and 5.13 ± 0.74 ms at FSN (circles, $n = 17$); the values are 1.12 ± 0.29, 3.58 ± 0.54, 5.46 ± 0.73, and 8.29 ± 0.94 ms at RSN (triangles, $n = 15$). The values from ISI_{1-2} to ISI_{4-5} are 35.72 ± 3.6, 41.1 ± 4.56, 47.56 ± 4.7, and 51.56 ± 4.84 ms at FSN (circles); the values are 38.57 ± 2.2, 53.89 ± 2.97, 64.34 ± 2.56, and 77.54 ± 3.84 ms at RSN (triangles). ISI and SDST relevant to the same number of sequential spikes are statistically lower at FSN than RSN ($p < 0.01$), except for spike one. These data indicate that FSN has higher ability in the programming of sequential spikes compared to RSN.

FSN expresses AHP (Fig. 1 and Ref. [28,30,31]). AHP mediated by the potassium channels and/or inhibitory synapses presumably influences the neuronal excitability and spike timing [6,20–26]. The data imply that AHP raises neuronal ability in programming spikes.

AHP improves spike capacity and timing precision

To address the role of inhibitory components in regulating spike programming, we injected depolarization pulses to evoke spikes and HP pulses (3 ms) immediately after each of spikes to simulate AHP. If HP pulses improve spike programming at RSN with no AHP, but not FSN with AHP, we are able to conclude that AHP is a critical factor in the improvement of spike programming. Fig. 2 shows the expression of spike capacity and timing precision at RSN (A–C) and FSN (D–F) without and with giving HP pulses.

Short-term HP pulses strengthen spike programming at RSN. Fig. 2B and C illustrates the quantitative analyses of ISI between spike one and two (ISI_{1-2}) up to four and five (ISI_{4-5}) as well as of $SDST_1$ to $SDST_5$. The values from ISI_{1-2} up to ISI_{4-5} are 17.2 ± 1, 31.5 ± 1.24, 37.87 ± 1.23, and 42.46 ± 1.42 ms under controls (opened triangles);

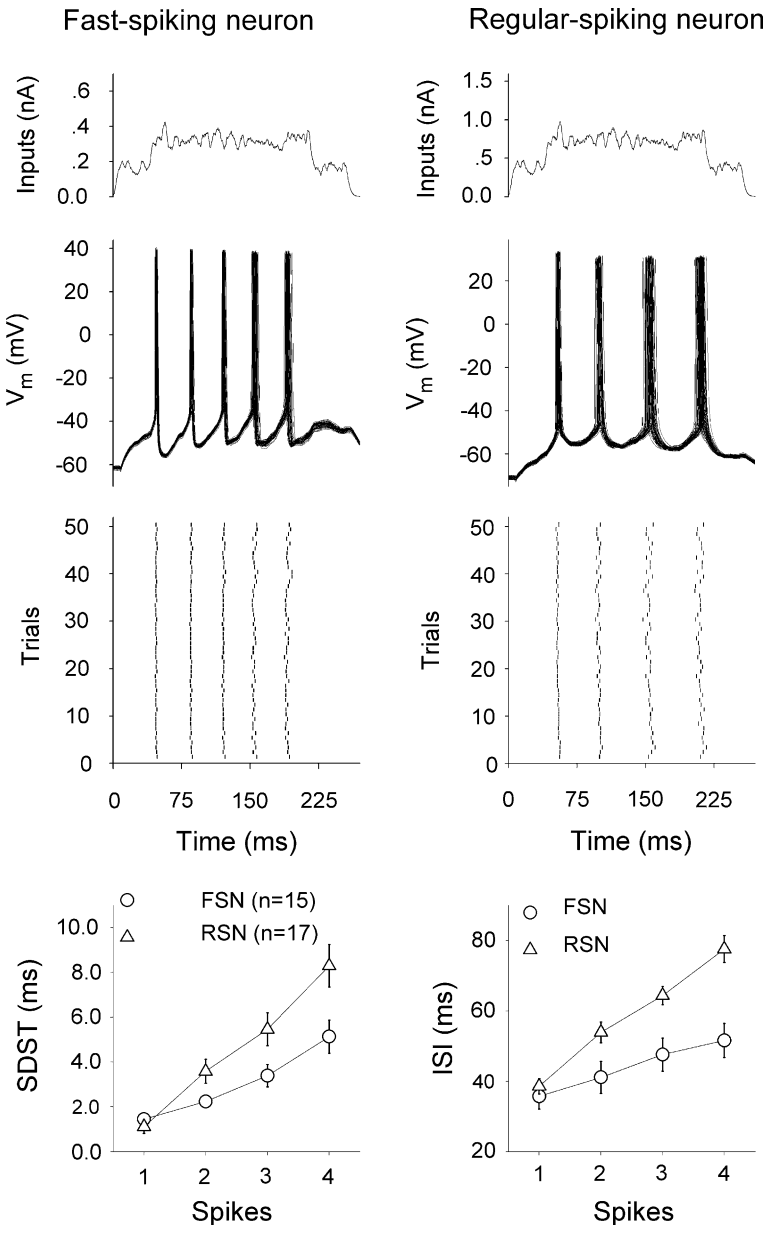

Fig. 1. The influences of excitatory inputs on spike capacity and timing precision in cortical fast-spiking (FSN) and regular-spiking neurons (RSN). Rows 1–3 from top to bottom represent the integrated currents, the evoked spikes superimposed from 50 traces, and the trials of spike timing at FSN (left panels) and RSN (right panels). The bottom row shows the statistical comparisons of the standard deviation of spike timing (SDST, left panel) and inter-spike intervals (ISI, right panel) vs. the number of spikes between FSN (circles, $n = 17$) and RSN (triangles, $n = 15$). FSN shows more dominant afterhyperpolarization (AHP) as well as lower SDST and ISI, i.e., better spike timing precision and capacity, compared to RSN ($p < 0.01$).

and the values are 17.63 ± 0.8, 27.88 ± 1, 32.12 ± 1.1, and 36 ± 1.55 ms under HP pulses (filled). The values for $SDST_1$ to $SDST_5$ are 0.35 ± 0.06, 0.68 ± 0.09, 1.36 ± 0.17, 1.8 ± 0.24, and 2.3 ± 0.34 ms under controls (open triangles); and values are 0.25 ± 0.03, 0.29 ± 0.03, 0.57 ± 0.06, 0.84 ± 0.13, and 1.03 ± 0.12 ms under HP pulses (filled triangles). SDST and ISI relevant to the same number of sequential spikes between controls and HP pulses are statistically different ($p < 0.01$, $n = 47$), except for spike one.

In FSN, short-term HP pulses improve spike timing only (Figs. 2D–F). The values from ISI_{1-2} to ISI_{4-5} are 24.9 ± 0.9, 26.7 ± 1.14, 28.4 ± 1.1, and 29.6 ± 1.2 ms under controls (opened circles); and the values are 23.2 ± 0.94, 25.8 ± 1.3, 27.5 ± 1.2, and 28.56 ± 1.26 ms under HP pulses (filled circles, $p > 0.05$, $n = 42$). The values from $SDST_1$ to $SDST_5$ are 0.37 ± 0.03, 0.65 ± 0.06, 0.95 ± 0.09, 1.3 ± 0.13, and 1.54 ± 0.16 ms under controls (opened circles); and the values are 0.29 ± 0.02, 0.41 ± 0.04, 0.54 ± 0.05, 0.67 ± 0.07, and 0.83 ± 0.1 ms under HP pulses (filled circles). SDST relevant to the same number of sequential spikes between controls and HP pulses are significantly different ($p < 0.01$, $n = 42$), except for spike one. The fact that natural AHP at FSN occludes

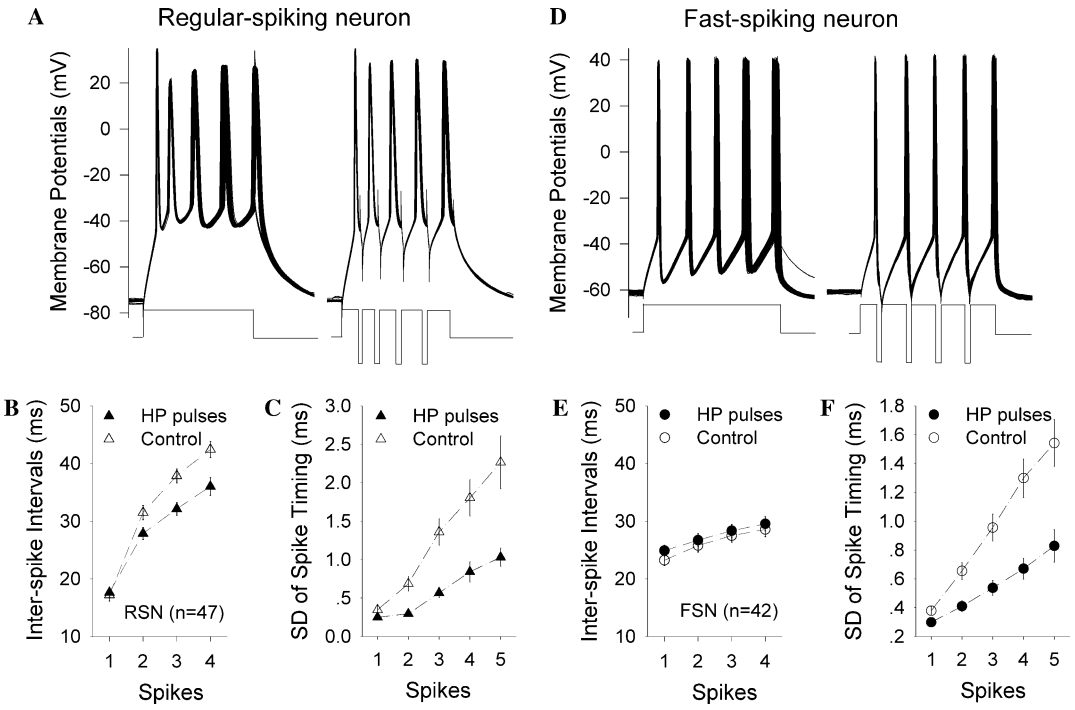

Fig. 2. The influences of inhibitory inputs on spike capacity and precision in cortical RSN (A–C, triangles) and FSN (E–F, circles). (A) Spikes, superimposed from 50 traces, evoked by a depolarization pulse (DP, 100–140 ms, left) and DP plus hyperpolarization pulses (HP, 3 ms, right) added after each spike. (B) The comparison of inter-spike intervals (ISI) after spikes 1–4 under control (open triangles) and HP (filled triangles, $p < 0.01$, $n = 47$). (C) The comparison of the standard deviation of spike timing (SDST) 1–5 under control (open triangles) and HP (filled triangles, $p < 0.01$, $n = 47$). (D) Spikes, superimposed from 50 traces, evoked by a DP (100 ms, left) and DP plus HP (3 ms, right) added after each spike. (E) The comparison of ISI after spikes 1–4 under control (open circles) and HP (filled circles, $n = 42$). (F) The comparison of SDST1-5 under control (open triangles) and HP (filled circles, $p < 0.01$, $n = 42$).

the effect of the simulated AHP on spike capacity implies that AHP improves spike programming in the sequence of spike capacity and timing precision, i.e., spike capacity is more sensitive to fast AHP.

FSN possesses low threshold potentials (Vts) and short refractory periods (RP) [27], which may be the reason for their high ability in spike programming (Fig. 1). The natural AHP at FSN improves spike programming (Fig. 2). Which factors are more important in improving spike programming? Does AHP affect spike patterns through its interaction with Vts and RP?

The influences of inhibitory currents on the threshold potentials of spikes

If AHP at FSN causes the lower Vts compared to RSN [27], HP pulses added immediately after each of spikes should bring Vts down significantly at RSN. Compared to DC pulse-evoked spikes (blue trace), HP pulses (3 ms) reduce the Vts-Vr of subsequent spikes at RSN (red trace in Fig. 3A). The values of Vts-Vr for spikes 2–5 are 35.32 ± 1.04, 36.57 ± 0.95, 36.46 ± 1.1, and 38.15 ± 1.26 mV under controls (open triangles); and the values are 32.3 ± 0.85, 33.11 ± 0.8, 33.37 ± 0.8, and 33.71 ± 0.78 mV under HP pulses (filled triangles). Vts-Vr values relevant to the same number of sequential spikes are lowered significantly by HP pulses ($p < 0.01$, $n = 15$, Fig. 3B). The fact that AHP lowers Vts at RSN indicates that inhibitory currents raise RSN sensitivity to excitatory synaptic inputs that drive membrane depolarization.

On the other hand, we observed that HP pulses immediately after each of spikes do not obviously lower Vts of sequential spikes at FSN (red trace in Fig. 3C). The values of Vts-Vr for spikes 2–5 are 27.1 ± 0.84, 27.69 ± 0.75, 28.2 ± 0.7, and 28.86 ± 0.74 mV under control (open circles); and the values are 25.9 ± 0.7, 25.8 ± 0.73, 26.41 ± 0.71, and 26.98 ± 0.7 mV under HP pulses (filled circles). Vts-Vr values relevant to the same number in sequential spikes 2–5 are not changed statistically by HP pulses ($p > 0.09$, $n = 17$, Fig. 3D). This result indicates that AHP at FSN occludes a role of HP pulses in lowering Vts, granting our prediction that AHP at FSN lowers its threshold potentials.

The influences of inhibitory currents on the refractory periods of spikes

FSN expressing AHP shows better spike programming compared to RSN (Fig. 1); and AHP improves spike timing (Fig. 2). If a mechanism underlying the effect of AHP at FSN is due to shortening RP, RPs should be shorter at FSN, as well as HP pulses should shorten RP at RSN. To test these predictions, we applied HP currents to hold

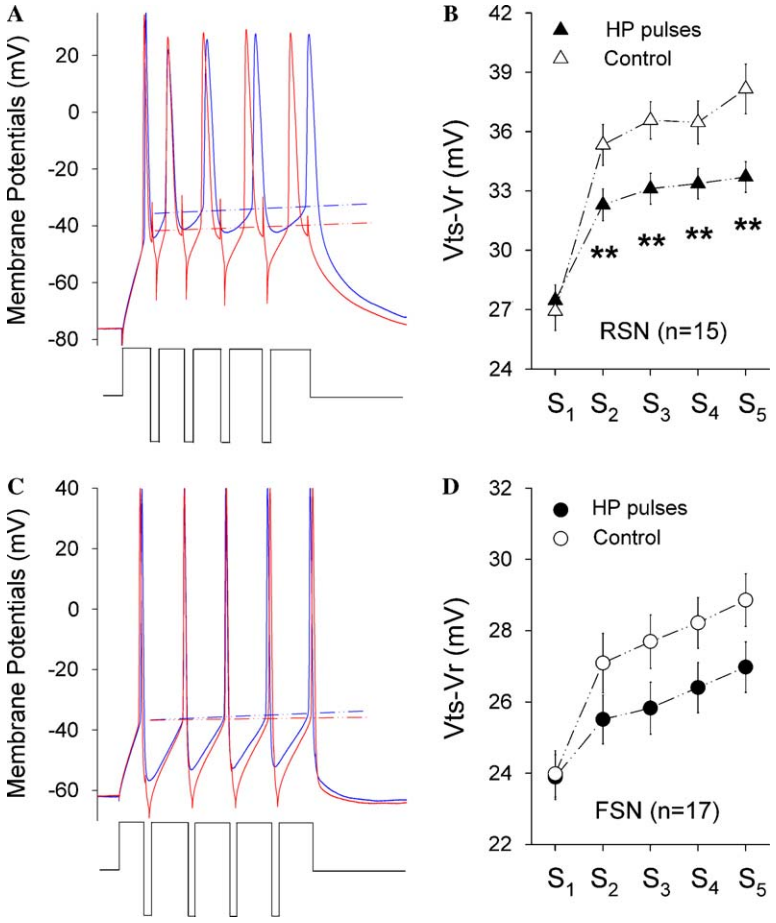

Fig. 3. Hyperpolarization pulses (HP) significantly lower the threshold potentials of the sequential spikes at cortical RSN (triangles), but not FSN (circles). (A) HP pulses subsequent to each of spikes shift threshold potentials from controls (blue trace) to low (red trace) at RSN. (B) HP pulses lower the Vts-Vr of spikes 2–5 at RSN (triangles; $n = 15$; $^{**}p < 0.01$. (C) HP pulses following each spike do not shift threshold potentials (blue trace in control and red trace in HP) at FSN. (D) HP pulses do not lower Vts-Vr of spikes at FSN (circles, $n = 17$; $p > 0.09$).

membrane potentials at hyperpolarization (10 mV) when measuring RP.

The absolute RP of sequential spikes were measured under conditions of resting membrane potential (Vr) and HP. Fig. 4A shows the recordings for ARP of spike 4 (ARP_4) at Vr (red trace) and 10 mV HP (blue), where HP appears to shorten ARP. The values of ARP_1–ARP_4 are 8.26 ± 0.32, 9.7 ± 0.41, 11.16 ± 0.45, and 12.78 ± 0.62 ms under Vr; and the values are 7.14 ± 0.28, 7.67 ± 0.25, 8.41 ± 0.35, and 8.8 ± 0.41 ms under HP at RSN ($n = 11$, Fig. 4B). In FSN, the values from ARP_1 to ARP_4 are 7.3 ± 0.36, 8.1 ± 0.36, 8.68 ± 0.4, and 9.21 ± 0.42 ms under Vr; are 6.35 ± 0.29, 6.75 ± 0.32, 7.1 ± 0.26, and 7.6 ± 0.4 ms under 10 mV HP ($n = 10$, Fig. 4C). The values of ARP relevant to the same number of sequential spikes at RSN or FSN under the conditions of Vr and HP are different significantly ($^{**}p < 0.01$; $^{*}p < 0.05$), i.e., a hyperpolarization shortens refractory periods.

If AHP shortens refractory periods, the hyperpolarization should dominantly affect ARP at RSN since FSN expresses AHP. Our analyses show that the net changes for ARP_1 up to ARP_4 between controls and HP are 1.12 ± 0.19, 2.03 ± 0.29, 2.75 ± 0.28, and 3.98 ± 0.6 ms at RSN; and their values are 0.93 ± 0.17, 1.29 ± 0.21, 1.57 ± 0.23, and 1.61 ± 0.44 ms at FSN (Fig. 4D). HP-induced ARP changes between RSN and FSN are different significantly ($^{**}p < 0.01$; $^{*}p < 0.05$), granting that the hyperpolarization shortens refractory periods.

Moreover, values for ARP_1–ARP_4 under control are 8.26 ± 0.3, 9.7 ± 0.4, 11.2 ± 0.45, and 12.78 ± 0.62 ms at RSN; and their values are 7.3 ± 0.36, 8.1 ± 0.36, 8.68 ± 0.4, and 9.21 ± 0.42 ms at FSN. ARP values relevant to the same number of sequential spikes are significantly lower at FSN with expressing AHP than RSN ($p < 0.01$). These results strongly suggest that inhibitory components shorten ARP of sequential spikes.

Hyperpolarization pulses facilitate the sequential activation of VGSC

If the Vts and ARP of spikes are controlled by VGSC activities, AHP should lower thresholds for VGSC activation and shorten refractory periods for its reactivation. To test this hypothesis, we recorded the currents of single VGSC by the cell-attached configuration without and with HP pulses, in which patch membrane was depolarized by

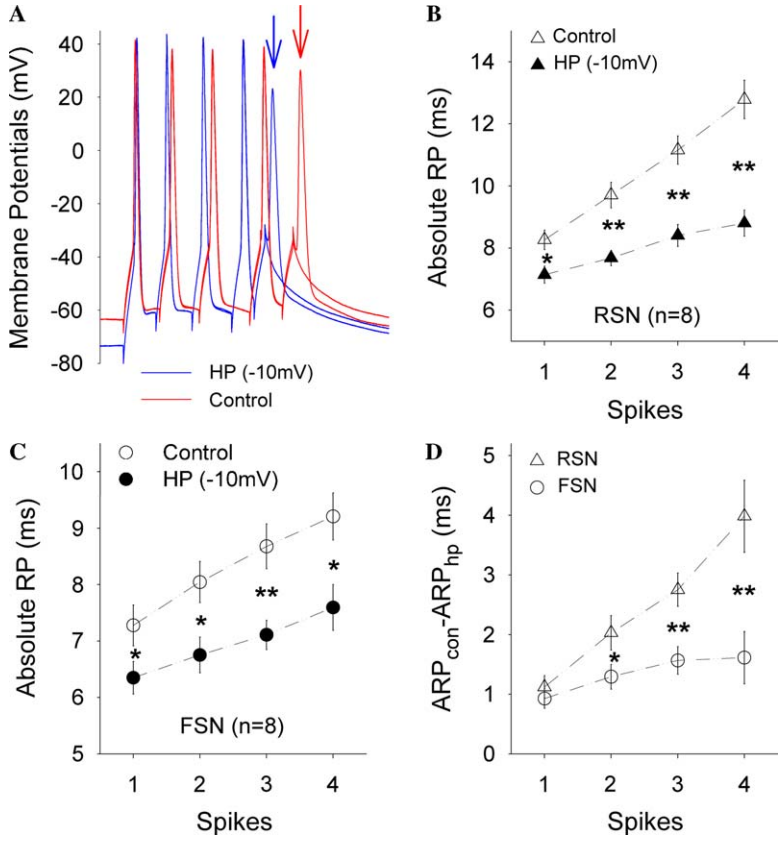

Fig. 4. Hyperpolarization shortens the refractory periods (RP) of sequential spikes at cortical RSN (triangles) and FSN (circles). (A) Traces show preliminary recordings that hyperpolarization (HP) shortens ARP (blue trace, −74 mV) compared to the resting membrane potential (Vr). (B) Quantitative data show the influence of HP (−10 mV, filled symbols) on ARP compared to Vr (−71 mV, open symbols) at RSN ($p < 0.01$). (C) The quantitative data show the influences of HP (−10 mV, filled symbols) on ARP compared to Vr (−63 mV, open symbols) at FSN ($p < 0.01$). (D) Net changes in RP values of the difference between control and HP for ARP_1–ARP_4 are different significantly ($p < 0.01$).

applying five depolarization pulses (DP, 15–40 mV/4 ms) to find the thresholds for VGSC activation and activity levels. As ARP for spike one is about 7–8 ms (Fig. 4), interpulse intervals (IPI) were set at 6–8 ms, which are used to identify refractory periods for VGSC reactivation. The intensity of pulses in Fig. 5 is 5 mV above the thresholds for VGSC activation.

Fig. 5 shows VGSC currents during sequential activations without and with AHP. The second pulse 6 ms after the first one (i.e., IPI_1 set at 6 ms) appears not evoking VGSC currents (Fig. 5A), whereas IPI_1 at 8 ms allows VGSC being reactivated (Fig. 5B). What IPI_1 for VGSC reactivation is between 6 and 8 ms, close to the range of spike ARP_1, implies that VGSC dynamics underlies ARP for spikes. Moreover, with IPI fixed at 6 ms, 20 mV HP pulses facilitate VGSC reactivation (Fig. 5C vs. A). Quantitative data are shown in Fig. 5D, where the hyperpolarization and longer interpulse interval make VGSC currents to be higher. These results indicate that the hyperpolarization pulses shorten the refractory periods for VGSC reactivation and lower the threshold potentials for its sequential activation, which in turn improve the programming of the sequential spikes.

Discussion

To test our hypothesis that afterhyperpolarization improves spike programming via VGSC-mediated intrinsic properties, we compared HP-induced plastic changes in the threshold potentials and refractory periods of sequential spikes at FSN and RSN. Spike Vts and ARP are lower at FSN that expresses fast AHP. HP pulses lower spike Vts and ARP dominantly at RSN (Figs. 3,4). HP pulses facilitate VGSC reactivation via lowering its thresholds and refractory periods. In addition to explaining why FSN is more sensitive to excitatory inputs, is highly excitable, and shows high ability in programming spikes [29,30 and Figs. 1,2], our results help understand the principles from neuronal intrinsic property to neural signal encodings.

Fast AHP [22] or a hyperpolarization via feedback inhibitory synapse after each of spikes [30–32] is expressed at certain neurons. Such hyperpolarization may affect neuronal excitability [6,21–26] and spike programming (Figs. 1,2). The mechanism underlying hyperpolarization-induced outcomes is based on the lowering of the threshold potentials (Fig. 3) to elevate the neuronal sensitivity to excitatory inputs as well as the shortening of refractory periods

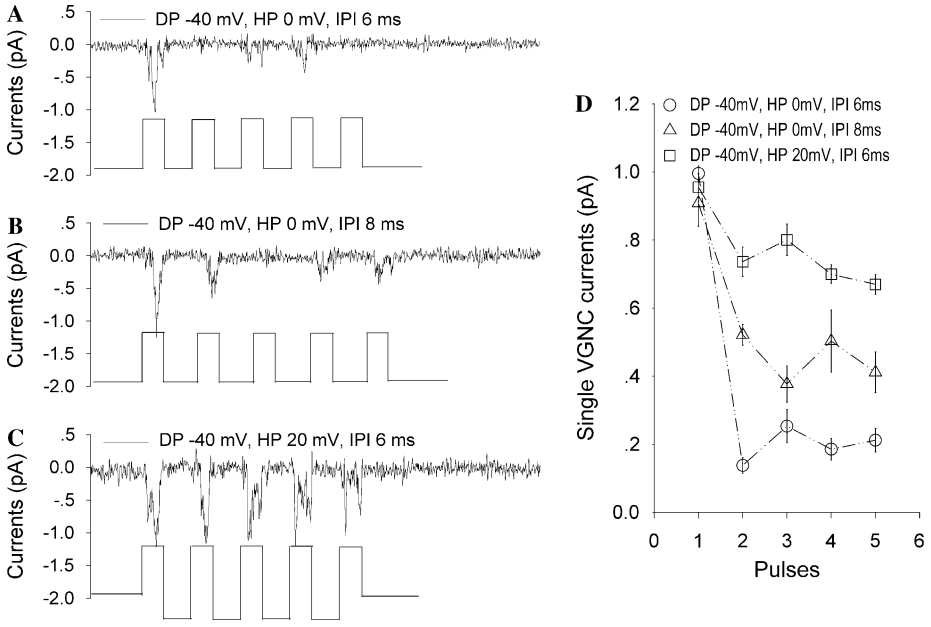

Fig. 5. Hyperpolarization pulses facilitate the sequential activations of VGSC. (A) VGSC activity under depolarization (DP) 40 mV and IPI 6 ms. (B) VGSC activity under DP 40 mV and IPI 8 ms. (C) VGSC activity under DP 40 mV, HP 20 mV, and IPI 6 ms. (D) Shows the quantitative data of VGSC activities under conditions in A–C ($n = 10$).

(Fig. 4) to allow subsequent spikes shifting toward front ones and raise spike capacity.

Spike timing is elicited more precisely by pulse depolarization (high variance input) than low variance input [21,33–36]. Variance current can be generated from the biphasic inputs of both excitatory and inhibitory synapses, or the sequential activation of sodium and potassium channels. The temporal and spatial summations of the excitatory components vs. inhibitory ones shape the fluctuation of membrane potentials. AHP lowers Vts (Fig. 3) and shortens ARP (Fig. 4); and stronger excitatory inputs facilitate VGSC sequential activations through lowering its ARP and Vts [37]. Thus, the hill of the fluctuated currents drives membrane potentials to be strongly depolarized, shortening ARP; whereas the valley shifts the membrane potentials toward the hyperpolarization, lowering Vts and ARP. What the high variance inputs improve spike programming is mechanistically caused by lowering threshold potentials and refractory periods.

The indications above grant a notion that the functional plasticity and anatomical weight of both excitatory and inhibitory inputs influence intrinsic properties and spike programming on the postsynaptic neurons. It is needed to address how excitatory and inhibitory synaptic inputs integrate quantitatively to encode neuronal signals precisely. It is believed that the activities of the excitatory synapses drive membrane potentials toward spike thresholds, whereas inhibitory synapses work oppositely [38]. Our data show that the inhibitory components immediately after spikes lower Vts and shorten ARP to enhance the firing ability at neurons, not simply suppressing neuronal activity. In this regard, the inhibitory inputs induce homeostatic processes in neuronal spike programming.

Voltage-gated sodium channel (VGSC) is activated by membrane depolarization to a threshold level and inactivated quickly; and its reactivation requires a sufficient repolarization or hyperpolarization [39]. The threshold potentials and refractory periods of spikes are presumably controlled by VGSC [40–43]. What AHP affects both the intrinsic properties of controlling sequential spikes and reactivation of VGSC in the same way at cortical neurons (Figs. 3–5) grants these notions. Our data also reveal that voltage sensor and gating controller in VGSC undergo the plasticity that is regulated by K-channel-mediated AHP in sequential spikes.

Additionally, as Vts in subsequent spikes shifts away from Vr (Figs. 1,2), each of VGSCs or some of them on cell membrane may not be completely recovered from inactivation when firing subsequent spikes though their refractory periods are over. In this regard, threshold potentials may more sensitively reflect the kinetics of VGSCs. Moreover, the values of Vts and ARP are lower at FSN than RSN (Figs. 3,4), implying that the dynamics of VGSCs on such two kinds of neurons is different, which is tested.

In summary, our studies indicate that the inhibitory components immediately after spikes lower threshold potentials and shorten refractory periods via influencing the dynamics of voltage-gated sodium channels. These changes make the neurons more sensitive to the driving of excitatory inputs for firing sequential spikes, i.e., improving the programming of sequential spikes that are digital language in the nervous system to guide well-organized behaviors.

Acknowledgments

This study is supported by National Awards for Outstanding Young Scientist (30325021), Natural Science Foundation of China (NSFC-30470362), NSFC (30621130077), Program for Hundred Gifted Scientists by Chinese Academy of Sciences, and National Basic Research Program (2006CB500804) to J.H.W.

References

[1] A.V. Anagnostopoulos, L.E. Mobraaten, J.J. Sharp, M.T. Davisson, Transgenic and knockout databases: behavioral profiles of mouse mutants, Physiology & Behavior 73 (2001) 675–689.
[2] G. Horn, Pathways of the past: the imprint of memory, Nature Review of Neuroscience 5 (2004) 108–120.
[3] C. Koch, Computation and the single neuron, Nature 385 (1997) 207–210.
[4] M. London, A. Schreibman, M. Hausser, M.E. Larkum, I. Segev, The information efficacy of a synapse, Nature Neuroscience 5 (2002) 332–340.
[5] M.N. Shadlen, W.T. Newsome, Noise, neural codes and cortical organization, Current Opinion of Neurobiology 4 (1994) 569–579.
[6] P. Somogyi, T. Klausberger, Defined types of cortical interneurone structure space and spike timing in the hippocampus, Journal of Physiology (London) 562 (2005) 9–29.
[7] N.C. Spitzer, P.A. Kingston, T.J. Manning Jr., M.W. Conklin, Outside and in: development of neuronal excitability, Current Opinion in Neurobiology 12 (2002) 315–323.
[8] P.H.E. Tiesinga, J.V. Toups, The possible role of spike patterns in cortical information processing, Journal of Computational Neuroscience 18 (2005) 275–286.
[9] D. Fricker, R. Miles, Interneuron, spike timing, and perception, Neuron 32 (2001) 771–774.
[10] R.S. Petersen, S. Panzeri, M.E. Diamond, Population coding in somatosensory cortex, Current Opinion of Neurobiology 12 (2002) 441–447.
[11] D. Daoudal, D. Debanne, Long-term plasticity of intrinsic excitability: learning rules and mechanisms, Learning & Memory 10 (2003) 456–465.
[12] W. Zhang, D. Linden, The other side of the engram: experience-driven changes in neuronal intrinsic excitability, Nature Review Neuroscience 4 (2003) 885–900.
[13] J.-M. Fellous, P. Tiesinga, P.J. Thomas, T.J. Sejnowski, Discovering spike patterns in neuronal responses, Journal of Neuroscience 24 (2004) 2989–3001.
[14] L.G. Nowak, M.V. Sanchez-Vives, D.A. McCormick, Influence of low and high frequency inputs on spike timing in visual cortical neurons, Cerebral Cortex 7 (1997) 487–501.
[15] S. Schreiber, J.-M. Fellous, P. Tiesinga, T.J. Sejnowski, Influence of ionic conductances on spike timing reliability of cortical neurons for suprathreshold rhythmic inputs, Journal of Neurophysiology 91 (2004) 194–205.
[16] A. Szucs, A. Vehovszky, G. Molnar, R.D. Pinto, H.D.I. Abarbanel, Reliability and precision of neural spike timing: simulation of spectrally broadband synaptic inputs, Neuroscience 126 (2004) 1063–1073.
[17] M.J. Berry II, M. Meister, Refractoriness and neural precision, Journal of Neuroscience 18 (1998) 2200–2211.
[18] B. Gutkin, G.B. Ermentrout, M. Rudolph, Spike generation dynamics and the conditions for spike-time precision in cortical neurons, Journal of computational neuroscience 15 (2003) 91–103.
[19] M.E. Mazurek, M.N. Shadlen, Limits to the temporal fidelity of cortical spike rate signals, Nature Neuroscience 5 (2002) 463–471.
[20] P.A. Glazebrook et al., Potassium channels Kv1.1, Kv1.2 and Kv1.6 influence excitation of rat visceral sensory neurons, Journal of Physiology (London) 541 (2002) 467–482.
[21] D. Hess, A.E. Manira, Characterization of a high-voltage-activated Ia current with a role in spike timing and locomotor pattern generation, Proceeding of National Academy of Sciences, USA 98 (2001) 5276–5281.
[22] D. Johnston et al., Dendritic potassium channels in hippocampal pyramidal neurons, Journal of Physiology (London) 525 (2000) 75–81.
[23] S. Nedergarrd, Regulation of action potential size and excitability in substantia nigra compacta neurons: sensitivity to 4-aminopyridine, Journal of Neurophysiology 82 (1999) 2903–2913.
[24] B. Rudy et al., Contributions of Kv3 channels to neuronal excitability, Annual New York Academy of Sciences 868 (1999) 304–343.
[25] P. Sah, Ca^{2+}-activated K^+ currents in neurones: types, physiological roles and modulation, Trends in Neuroscience 19 (1996) 150–154.
[26] M. Wehr, A.M. Zador, Balanced inhibition underlies tuning and sharpens spike timing in auditory cortex, Nature 426 (2003) 442–446.
[27] N. Chen, S.L. Chen, Y.L. Wu, J.H. Wang, The measurement of threshold potentials and refractory periods of sequential spikes by whole-cell recordings, Biochemical and Biophysical Research Communications 340 (2006) 151–157.
[28] B.W. Connors, M.J. Gutnick, Intrinsic firing patterns of diverse neocortical neurons, Trends in Neuroscience 13 (1990) 99–104.
[29] J.-H. Wang, Short-term cerebral ischemia causes the dysfunction of interneurons and more excitation of pyramidal neurons, Brain Research Bulletin 60 (2003) 53–58.
[30] T.F. Freund, G. Buzsaki, Interneurons of the hippocampus, Hippocampus 6 (1996) 347–470.
[31] A. Sik, A. Ylinen, M. Penttonen, G. Buzsaki, Inhibitory CA1-CA3-hilar region feedback in the hippocampus, Science 265 (1994) 1722–1724.
[32] R. Gutierrez, The dual glutamatergic-GABAergic phenotype of hippocampal granule cells, Trends in Neuroscience 28 (2005) 297–303.
[33] N. Axmacher, R. Miles, Intrinsic cellular currents and the temporal precision of EPSP-action potential coupling in CA1 pyramidal cells, Journal of Physiology (London) 555 (2004) 713–725.
[34] J.M. Fellous et al., Frequency dependence of spike timing reliability in cortical pyramidal cells and interneuron, Journal of Neurophysiology 85 (2001) 1782–1787.
[35] Z.F. Mainen, T.J. Sejnowski, Reliability of spike timing in neocortical neurons, Science 268 (1995) 1503–1506.
[36] Y. Shu, A. Hasenstaub, M. Badoual, T. Bal, D.A. McCormick, Barrages of synaptic activity control the gain and sensitivity of cortical neurons, Journal of Neuroscience 23 (2003) 10388–10401.
[37] N. Chen, Y. Zhu, X. Gao, S. Guan, J-H. Wang .Sodium channel-mediated intrinsic mechanisms underlying the differences of spike programming among GABAergic neurons. Biochemical and Biophysical Research Communications Accepted (2006).
[38] E.R. Kandel, S.A. Siegelbaum, J.H. Schwartz, in: E.R. Kandel, J.H. Schwartz, T.M. Jessell (Eds.), Principles of Neural Science, McGraw-Hill, New York, 2000, pp. 175–308.
[39] B. Hille, The Superfamily of Voltage-Gated Channels, Sinauer, Sunderland, MA,, 2001, 1-61-93.
[40] R. Azous, C.M. Gray, Dynamic spike threshold reveals a mechanism for synaptic coincidence detection in cortical neurons in vivo, Proceeding of National Academy of Sciences, USA 97 (2000) 8110–8115.
[41] A.R. Cantrell, W.A. Catterall, Neuromodulation of Na^+ channels: an unexpected form of cellular plasticity, Nature Review Neuroscience 2 (2001) 397–407.
[42] C.M. Colbert, E. Pan, Ion channel properties underlying axonal action potential initiation in pyramidal neurons, Nature Neuroscience 5 (2002) 533–538.
[43] M.C. Kiernan, A.V. Kirshnan, C.S. Lin, D. Burkke, S.F. Berkovic, Mutation in the Na^+ channel subunit SCN1B produces paradoxical changes in peripheral nerve excitability, Brain 128 (2005) 1841–1846.